SYNTHESIS AND CHARACTERIZATION OF MESOPOROUS MATERIALS AND THEIR APPLICATIONS IN FINE CHEMICAL SYNTHESIS

A THESIS

SUBMITTED TO THE

UNIVERSITY OF PUNE

FOR THE DEGREE OF

MASTER OF SCIENCE (M.Sc)

(PARTLY BY PAPER AND PARTLY BY RESEAERCH)

IN

CHEMISTRY

BY

RATNESH KUMAR JHA

CATALYSIS DIVISION
NATIONAL CHEMICAL LABORATORY
PUNE – 411 008, INDIA.

SEPTEMBER - 2005

CHAPTER I
INTRODUCTION

1.1. General Introduction

Catalysis may well be one of the most practical of the many sub disciplines of physical science and had emerged as an important field which combines applied science with technology, as most of the valuable things for human needs can be achieved through catalytic reactions. In practice, catalysis is primarily a technology that draws on many fields such as organic chemistry, surface chemistry, chemical kinetics, thermodynamics, solid states, physics ceramics and physical metallurgy and so the term an interdisciplinary subject seems to be very aptful [1]. Even though J. J. Berzelius introduced the term catalysis in 1836, the definition seems to get modified as the surface properties and the ideas of what constitute a catalyst and mechanism for catalytic activity have undergone continuous refinement, and Ostwald scientifically defined the term catalysis firstly in 1894. According to Ostwald, "Catalysis is the phenomenon in which a small quantity of substance, the catalyst increases the rate of reaction or the rate of approaching the equilibrium of a chemical reaction without itself being substantially consumed"[2]. It was not until the start of 20^{th} century that scientific observation border crossing i.e., inter disciplinary occupation (viz. organometallic chemistry, material sciences, physical chemistry, and chemical engineering) and surface sciences enlarged the knowledge of catalysis and catalysts considerably. In general, a catalyst can be defined as a substance that increases the rate of reaction towards equilibrium without being appreciably consumed in the process.

In a bulk of various possible reactions a given catalyst will not catalyze equally all or several of the possible pathways, thus offering an elegant method for directing conversions in the desired course and velocity i.e., partial or selective conversions. In the majority of catalytic processes used industrially, the products are not those expected for full conversions. This feature of catalysis whereby reactions can be tuned on to unusual pathways, with tremendous acceleration of reactions, greatly enhances its value and makes it a thoroughly fascinating branch of science. Innovations in catalysis have minimized usage of energy and raw materials and will become of increasing importance for the production of chemicals and in the drive to minimize environmental wastage. Catalysis focuses mainly on three aspects - the catalyzed reactions (often organic), the inorganic chemistry of catalyst preparation and catalyst characterization.

Catalysis has been an intriguing concept and continuing efforts have been done to understand and utilize the phenomenon for practical purposes. This has resulted in numerous inventions during this century, which have been responsible in improving the quality of human life, so the recent catalysis research is focused in achieving 100% selectivity for the desired product in all catalyst based processes which provides both economic and environmental benefits [3]. Nearly 95% of all processes used in chemical industry are catalyst based and a large part of these transformations are performed with the homogeneous metal species, which produces stoichiometric amounts of unwanted toxic byproducts. Hence it is necessary for the chemical industry and technologists for a better alternative for environmental protection and so nowadays a green methodology is emerging for the catalyst synthesis for industrially important compounds. This will

provide a concept of green chemistry, which will enable a clean manufacturing with no generation of wasteful or polluting by-product.

Catalysts are divided broadly into two groups as homogeneous and heterogeneous. A catalyst is named homogeneous, when the catalyst and reactant are in same phase, i.e. either in gaseous or in liquid phase. The advantages of homogeneous catalyst lies in the fact that every catalyst molecule become accessible to the reactant, since it dissolve in a liquid phase and so catalysis is more efficient. Secondly molecular catalyst design can be used to effect better control of selectivity and mass and heat transfer problems associated with the heterogeneous catalyst can be avoided. Although homogeneous catalyst are effective for various reaction like hydrogenation, isomerisation, oxidation-reduction they are not employed industrially because of its toxic nature, requirement of stoichiometric amounts of catalysts and in its difficulty to separate from the product mixture [4].

Heterogeneous catalysis has been the basis for most of the commercial process for its technological applications. It is related to the diverse branches of science including chemical kinetics, thermodynamics, mass and heat transfer, solid-state physics and surface chemistry. But in homogeneous catalysis as the catalyst is molecularly well dispersed, every catalyst molecule will become accessible to the reactant, so catalysis is efficient and thus the mass and heat transfer problems associated heterogeneous catalyst can be avoided. However stoichiometric amounts of catalyst and its difficulty to separate from the product mixture, along with the expensive regeneration make the process economically non-viable. To explore the merits of homogeneous catalysts, research scenario had drawn considerable attention towards the heterogenisation of various value

added homogeneous catalyst and as a result the frontier between these two classes become much narrowed.

1.2. Molecular sieves as catalysts

Molecular sieves are the channel pores and aperture whose dimensions are approximately equal to those of many of the molecules converted in catalytic process. Since these materials selectively pass products of a definite orientation the term molecular sieves can be used and now a days these materials are well used in the field of separation science and especially in the field of catalysis as stable supports In the overwhelming majority of heterogeneous catalytic reactions, the chemical reaction is limited to the interface between solid and liquid phase and a preferable way to improve catalytic activity is to have large catalytically active surface area exposed to the reaction medium, since catalytic activity and surface area are directly related. The porous solid materials classified as a function of pore diameter are [5],

a) Microporous materials [d<20 Å]
b) Mesoporous materials [20<d<500 Å]
c) Macroporous materials [d> 500 Å].

Some materials such as zeolites and many clay minerals are entirely microporous than the irregular pores with widely variable pore diameters and in the conventional silica gel/alumina. The intra crystalline space in zeolites, which is commonly regarded as

system of micropores, have the common property of selectively sorbing molecules and thus offers most useful selectivity, thus come under the class of molecular sieves [6,7]. In catalyst industry zeolites are the most widely used microporous molecular sieves. They are crystalline microporous materials, which have become extremely successful as catalysts for oil refining, petro chemistry and for the production of various fine and specialty chemicals. Among various zeolites, faujasite, mordenite and ZSM-5 types are widely used, where the catalytic activity arise mainly due to their acidic nature. However, a variety of trivalent (B, Ga, Fe, As) [8-11] and tetravalent (Ti, V, Cr, Sn, Zr) [12-17] transition and non-transition metal ions have introduced in a variety of different zeolite structures for their well application in the redox catalysis.

1.3. Applications of mesoporous materials

Despite the enhanced catalytically desirable properties, the pore dimensions (5-7 Å) of zeolites are not sufficient to accommodate the broad spectrum of larger molecules for the various catalytic transformations. The performance of zeolitic system is limited by diffusional constraints associated with small pores. To a certain extent it is possible to overcome this problem with aluminophosphates (ALPOs) [18,19], microporous crystalline materials with pore dimensions up to 13 Å their limited thermal stability as well as negligible catalytic activity due to frame work neutrality makes them the least interesting. Moreover the need for present day heterogeneous catalyst in processing hydrocarbon with high molecular weight made researchers to think for better alternative to zeolites and these led to the discovery of mesoporous materials with large

surface area and higher pore diameters. Hence there has been an overgrowing interest in expanding pore sizes of zeolitic materials from micro pore to mesopore region.

1.4. Ordered mesoporous silica materials

Constructing solids with expected porous texture and architecture is one of the challenging tasks for researchers all over the world, as the apt design of a porous material can well tune the selectivity for a desired product in a specified reaction. The advent of supramolecular chemistry had given a new thrust to this field of porous solids by the announcement of the formation of mesoporous silicate and aluminosilicate molecular sieves with liquid crystal templates by the researchers at Mobil Research and Development Corporation in 1992 [20,21]. This family of materials generally called M41S molecular sieves consists of one-dimensional hexagonal MCM-41, three-dimensional cubic MCM-48 and lamellar MCM-50. These mesoporous materials with well defined pore sizes of 15 – 100 Å**,** and higher surface areas (>1000 m^2/g) break past the pore size constraint (15Å) of microporous zeolites. The synthesis of M41S materials thus paves an explosion of new investigations in the synthesis procedures, synthesis mechanisms, heteroatom insertion, characterization, adsorption and in catalytic reactions [22-26].

1.5. Mechanisms of mesostructure formation

In order to explain the formation of mesoporous materials and to provide a rational basis for the various synthesis routes a number of models have been proposed.

These models are predicted upon the presence of surfactants in a solution to guide the formation of the solubilized inorganic precursors. Surfactants contain a hydrophilic head group and a long hydrophobic tail group within the same molecule and self organize in such a way as to minimize contact between incompatible ends. The type of interaction between surfactant and inorganic precursor results in various synthesis routes, formation models and the resulting classes of mesoporous materials.

1.5.1. Liquid Crystal Templating Mechanism

A liquid crystal templating (LCT) mechanism was proposed by the Mobil researchers, based on the similarity between liquid crystalline surfactant assemblies [27,28] (i.e., lyotropic phase) and M41S [21]. The mesoporous structure depends on the length of the hydrocarbon chain, surfactant head group, the effect of variation of surfactant concentration and the influence of organic swelling agents. At low concentration, the surfactant molecules exist as randomly dispersed mono molecules in aqueous solution. With increasing concentration surfactant molecules aggregates with their hydrophobic tails together exposing their polar heads to aqueous solution to reach minimum energy configurations. The lowest concentration at which surfactant molecules aggregate to form spherical isotropic micelle is called critical micelle concentration (CMC-1). Further increase in surfactant concentration initiates aggregation of spherical into cylindrical or rod like micelles (CMC-2). Among the three crystalline phases of M41S materials, the hexagonal phase is the result of packing of cylindrical micelles, the lamellar phase corresponds to formation of surfactant bilayers

and cubic phase may be regarded as a bicontinuous structure. Two mechanistic pathways were postulated to understand the formation of mesostructure. (Scheme 1)

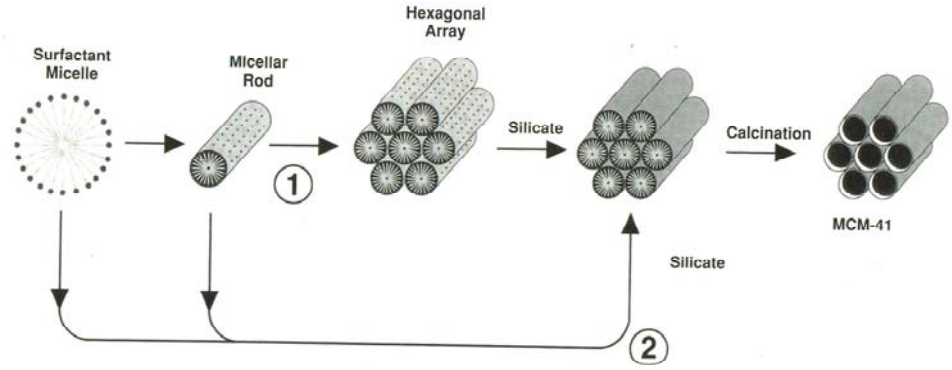

Scheme 1

i) The structure is defined by the organization of surfactant molecules into liquid crystals, which serve as template for the formation of the MCM-41 structure. The first step in the synthesis would correspond to the formation of micellar rod around the rod like structures that in a step would produce a hexagonal array of rods, followed by the incorporation of inorganic array around the rod like structures.

ii) The inorganic species mediated, in some manner, the ordering of the surfactants into the hexagonal arrangement.

In either case, the inorganic components that are negatively charged at high pH conditions, interacts strongly with cationic surfactants and the subsequent condensation followed by polymerization leads to mesostructure. However pathway 1

did not take place because the surfactant concentrations used were far below critical micelle concentration (CMC2) required for hexagonal LC formation [29].

1.5.2. Silicate Rod Assembly

Davis et al. [30] by carrying out *in situ* ^{14}N NMR spectroscopy, found that the LC phase is not present in the synthesis medium during the formation of MCM-41. They proposed that under synthesis conditions suggested by Mobil for the formation of MCM-41 randomly ordered rod like micelle interact with silicate species to yield two or three layers of silica around the external surface of micelle to yield tubular silica deposited micelle rods. The silicate encapsulated rods, which are randomly ordered, pack to hexagonal mesostructure. Heating and aging complete the condensation of silicate into the as synthesized MCM-41 structure. (Scheme 2)

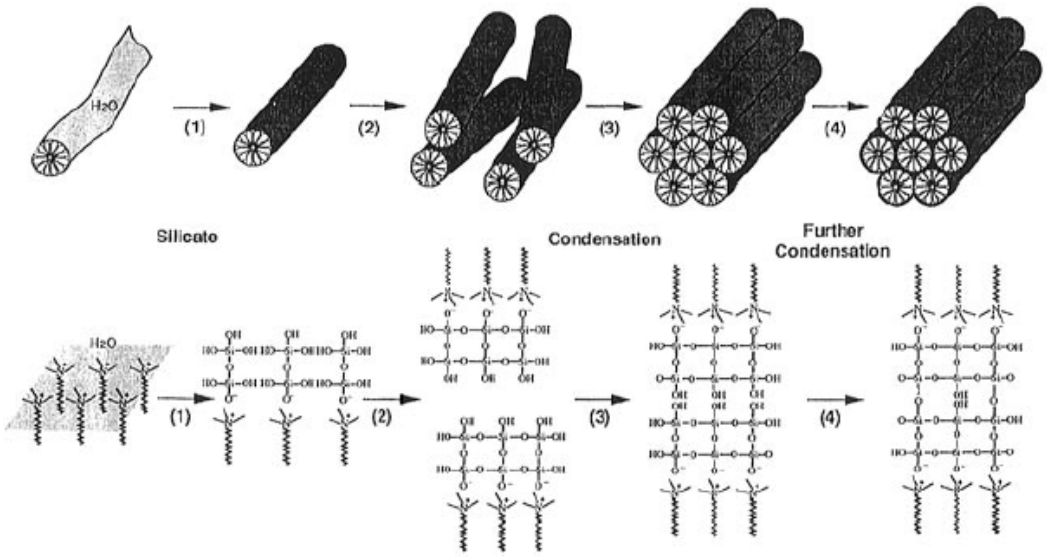

Scheme 2

1.5.3. Silicate Layered Intermediate

Steel et al. [31] postulated that surfactant molecules assembled directly into the hexagonal LC phase upon the addition of the silicate species based on ^{14}N NMR spectroscopy, instead of the formation of silicate covered micellar rods. The silicates were ordered into layers, with rows of cylindrical rods interacted between the layers. Aging the mixture caused the layers to pucker and collapse around the rods, which results in hexagonal phase. Monnier et al. [32] and Stucky et al. [33] postulated a charge density matching model and they suggested that MCM-41 can be derived from a lamellar phase. This is a three-step mechanism. In the first step, the oligomeric silicate polymers act as multidentate ligand for the cationic surfactant head groups leading to strongly interacted surfactant – silica interface with the lamellar phase. In the second step preferential polymerization of silicate occurs at the interface, so that charge density was reduced. To maintain charge density balance with surfactant head groups, curvature was introduced into the layers, which transformed the lamellar structure into hexagonal structure.

1.5.4. Silicatropic Liquid Crystals

Firouzi et al. [34] found that at low temperature and high pH (~ 14) a true co-operative self assembly of the silicates and the surfactants takes place, in which a lamellar solution of surfactant is transformed into a hexagonal phase in the presence of silicate anions (Scheme 3). Heating of this would lead to the formation of mesostructure materials.

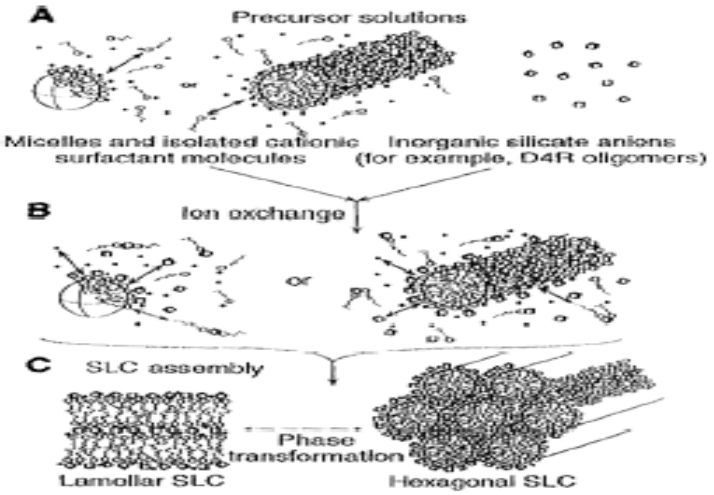

Scheme 3

1.6. Interaction between surfactants and silicate species.

When a silica source is combined with an ionic surfactant like CTMABr in solution the self-organization process involves surfactant/silicate self-assembly and the transformation of mesophase. Scheme 4, shows the aggregation process driven by the silica species and these are very sensitive to pH, temperature, aging time, counter ions and the surfactant species. In the synthesis there are three kinds of charged species in solution: Silica species (I^-/I^+), cationic surfactant (S^+) and its counter ion (X^-). Their interactions depend on the silicate oligomeric species present because their charge density is different in the degree of oligomerisation. With strong interactions the silicate ions exchange on to the micellar interface and the concentrations results in a rapid condensation of the silicate species.

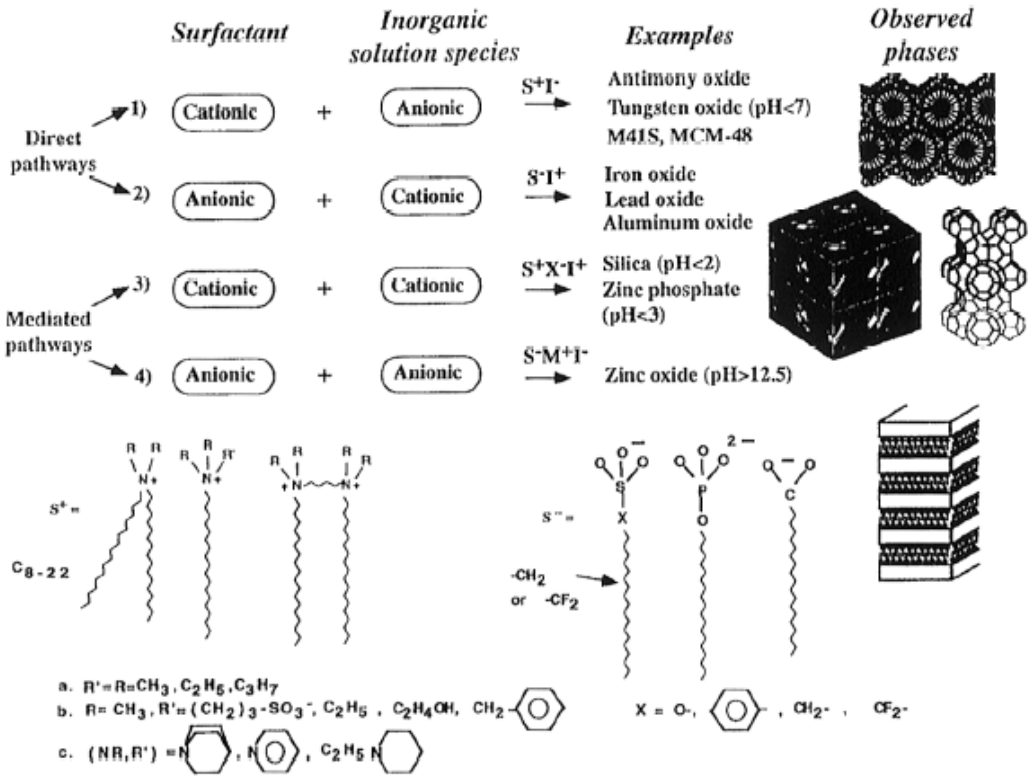

Scheme 4

1.6.1. Changes in acidity with polymerization

The hydrolysis and condensation rate of the silica species are pH dependant. If the pH is lower than the isoelectric point of silica, then the condensation is acid catalyzed and becomes faster as the pH decreases [35]. At pH >2 the condensation rate increases with pH until 8 and then decreases again. In a specially designed alkaline synthesis of MCM 41 the initial pH of silicate solution is fairly high (pH=11-12) which leads to highly charged anionic silicate species in solution and a lower rate of condensation. It has the advantage of separating silicate-surfactant (SS) assembly and silica condensation. The initially homogeneous SS solution can phase- separated into a lyotropic crystalline phase, which leads to different hierarchical structures. This is possible because of the low extent

of silica condensation in the surfactant-silicate assembly. After the structure is formed, "delayed way of neutralization" brings down the pH in the range of 8 without the formation of any amorphous silica phase. The lower pH leads to further silica condensation and thus leads to mesoporous materials with thicker walls [36]. Indeed the pH is low enough; otherwise calcinations of the materials may cause a collapse in the mesostructure [37].

1.6.2. Alkaline synthesis of mesoporous silica

In alkaline surfactant-silicate assembly equilibrium can be shifted by the presence of other ionic species in solution. This mean that the salt can effect the screening of the surfactant charge and hence the structure of the assembly. In the synthesis mixture, silicate polymerization can occur either at the surfactant/water interface or in solution. The competition with the X^- anions to bind with micelles depends on the relative binding ability of silicate anion species with respect to counter ion. Xios et al., [38] made mesoporous silica with hexagonal structure possessing high acidity and hydrothermal stability. They used TEAOH to separately develop a zeolytic nanocluster as silica precursor to make the mesoporous materials with cationic surfactant.

1.6.3. Acidic synthesis of mesoporous silica

In acidic media (pH<2), the positively charged silica oligomers cannot combine directly with positive surfactant and for charge balance, there must exist a bridge conterion (X^-) at the interface of silicas and surfactants. In acidic synthesis, the silica is usually less condensed and the structure order is thus softer and often leads to rich

morphologies (such as film, fiber, and gyroid) [39,40]. In acidic synthesis one can involve the surfactant mesophase first and then use the structure as a template. Because of the weaker surfactant-silicate interaction the original liquid crystalline phase can be preserved when mixing with silica sources

1.7. Modification of Mesoporous Materials

As synthesized mesoporous materials are catalytically inactive due to their framework neutrality. Modification of mesoporous materials can lead to the generation of acidic and basic properties and also leads to alteration of redox properties. So to get desired catalytic activity for a particular reaction, the catalyst should be modified by incorporating metal or acidic or basic components because these additives suppress undesirable side reaction by adjusting the acid base properties of the catalyst, and promote desirable reactions with their versatile active sites. Modification of M41S can be as follows.

i) Acidic properties can be created by incorporation of group +3 cation. B, Al, Ga-substituted MCM-41 (B,Al,Ga-MCM-41) having large pores with acidity on the walls were used to be in catalytic cracking, alkylation etc.

ii) If acidity is generated, the basicity of conjugate base can be increased by exchanging protons by alkaline ions. This mild basicity is useful for less demanding base, catalyzed reactions.

iii) The incorporation of transition metals like Ti^{4+}, V^{5+}, Cr^{6+} on the walls will generate redox properties. They are useful in selective oxidation of large organic molecules as well as pollution abatement.

iv) The M41S materials can act as support for the heterogenisation of homogeneous catalysts, for the deposition of metal oxides etc.

1.8. Synthesis of metal containing mesoporous materials

The general procedures for the formation of metal incorporated ordered mesoporous material is by a direct method and by post synthesis modification the mesoporous support.

1.8.1. Metal substituted mesoporous molecular sieves

The possibility of introducing heteroatom in the inert framework or walls of purely siliceous mesoporous materials by isomorphous substitution is an important route to modify the nature of framework and make them catalytically active through direct in situ method. Indeed the direct synthesis can be performed in two ways – one by the hydrothermal way in an autoclave and the other by using a reflux method at atmospheric pressure under stirred condition. In this method, the required amount of metal precursor salt dissolved in an appropriate solvent was added to the surfactant – silicate mixture and was aged for the desired time for incorporation of metals on the silica framework. The incorporation of trivalent metal ion such as Al, B, Ga, Fe, [41-44] etc. in the walls of

silica network mesostructure produces framework negative charges that can be compensated by protons producing acid sites and therefore such materials are important from the point of view of acid catalysis. The incorporation of transition metals such as Ti, V, Cr, Mn, [45-48] etc. is also important to prepare mesoporous catalysts with redox catalytic properties.

1.9. Removal of template

Removal of template plays a crucial role in the preparation of molecular sieves. Depending on the preparative method, in general template can be removed by calcination in air or by solvent extraction. However it has been observed that calcination is the better way than removal by extraction techniques. This is due to the strong interaction between template and inorganic species in the case of direct pathways or mediated pathways where electrostatic interaction plays a key role for the formation of mesostructure. The calcination has to be done in the flow of inert gases at the initial stages followed by the flow of air. This is to maintain the crystallinity of the material but extraction prefers when we need maximum hydroxyl group in the catalyst.

1.10. Applications of ordered mesoporous materials

First obvious applications of ordered mesoporous materials were seen in catalysis where a need for zeolitic like materials with bigger pore sizes was identified to process heavier residues more efficiently. The unique physical properties have made these materials highly desirable for catalytic applications. For catalysis, one of the major points is the high surface area of MCM-41 and all related materials, which can be

exploited for depositing metals, incorporating metals in the walls, or grafting species to the walls. A second beneficial feature of ordered mesoporous oxides in catalysis could be the sharp pore size distribution, which is reminiscent of zeolites and thus suggests applications in shape selective reactions. Metal substituted mesoporous molecular sieves have been investigated as catalysts for oxidation reactions, acid catalyzed reactions, hydroxylation reaction, polymerization reactions, etc. Metal deposited mesoporous silicates find applications in gas oil cracking, reduction of nitrogen oxides from emission gas, de-metallation of hydrocarbon feedstock, oligomerisation reactions, isomerisation reactions, hydrogenation, acid catalysis, base catalysis, coupling reactions, etc [25].

Apart from catalysis, other application fields seem to be quite promising. The well-defined mesoporous M41S also offer interesting potential for use in membrane separation, adsorption and electronic/optical applications [55]. The huge pore volume and the compositional flexibility of MCM-41 type materials are widely exploited for the selective adsorption of gases liquid and binding of metals. The modification of internal surface of MCM-41 with organo modifiers results in materials having excellent binding behavior for heavy metals, which was far superior to commercial adsorbents [56]. The low refractive index and low dielectric constant lead to their use in technical devices in electronic industry.

1.11. Oxidation catalysis

In earlier days, for the synthesis of value added compounds, oxidation was carried out using powerful oxidizing agents like $KMnO_4$, $K_2Cr_2O_7$ etc. in stoichiometric

quantities, generating a large amount of reduced products of these materials. Thus the oxidation reactions involving catalytic amount of oxidizing agent have come into prominence. Catalytic oxidation includes the processes of the petrochemical industry- selective oxidation, oxidative dehydrogenation (ODH), oxychlorination, ammoxidation, epoxidation and ammoximation, inorganic chemicals industry - oxidation of SO_2 and NH_3 for the manufacture of H_2SO_4 and HNO_3, fine chemicals industry- hydroxylation, acetoxylation, oxidation of carbohydrates, refinery industry, energy production- methanation, catalytic combustion in gas turbines and fuel cells and technologies for the protection of environment- automotive exhaust catalyst, catalytic oxidation of volatile organic compounds, catalytic combustion and combustion of organic matter.

In catalytic oxidation the choice of oxidant is influenced by both economic and environmental conditions [57,58]. The primary oxidant should preferably contain a high percentage of active oxygen and afford a co-product that is innocuous and/or easily recyclable. Oxidants that meet these criteria are oxygen, hydrogen peroxide (H_2O_2) and alkyl hydro peroxides such as TBHP. One of the reasons for the catalytic importance of metal catalysts is that bonding between reacting molecules and metal surface is such that interaction is weak enough for the product molecules to desorb, but strong enough for the reactant molecules to adsorb and rearrange upon chemisorption. Metal catalyzed oxidations with H_2O_2 and RO_2H can involve homolytic pathways via free radical (HO*, HO2*, RO*, RO2*), intermediate or heterolytic oxygen transfer process. The latter can proceed via oxometal or peroxometal species as the active oxidant [58].

1.12. Liquid phase redox reactions

With the incorporation of transition metal ions in the framework of silicate molecular sieves, an increasing attention is being paid to oxidation reactions. In every oxidation reactions two reactants take part, the oxidant and the hydrocarbon molecule to be oxidized. One of the major recurring problems encountered in liquid phase heterogeneous organic transformations is the reaction between mutually immiscible reagent(s) and substrate. If the chemical reaction takes place at the liquid – liquid phase boundary, rapid stirring may have an accelerating effect by increasing the interfacial contact [59]. Alternately, the addition of co-solvent can bring about a homogeneous state and thereby completely eliminating the phase boundaries. There are certain reactions on which the conversion of the substrate to the corresponding oxidized products occurs only with the presence of co-solvents. In such reactions, the amphiphilic solvent used increases the rate of diffusion of reactants to the active sites of the catalyst and also the rate of diffusion of products from the catalyst surface. The solvent is chosen in such a manner that the reactants and products must be soluble it. The system consisting of one solid phase, i.e., catalyst and another liquid phase consisting of organic substrate and aqueous oxidant in co-solvent to homogenize the liquid layers are referred to as biphasic systems.

Even though, the use of co-solvents often found its utility [60], product separation suffers from the drawback of complex work-up procedure. To overcome this problem phase transfer catalysts are used [61,62]. The use of solid catalyst, where the phase transfer catalysts were generally anchored/grafted in a polymer or inorganic

supports [63,64] and the catalyst is sandwiched between organic and aqueous layers is also reported. But they also suffer from the problem of complex work-up. The system in which, solid catalyst along with two mutually immiscible reactants makes up the triphasic reaction system. The three phases consisting of solid catalyst, water immiscible organic substrate and aqueous oxidant were physically non-interacting in nature. In such systems the hydrophilic/hydrophobic nature of the catalyst plays a key role in enhancing reaction rate and selectivity. The reactions occurring in biphasic and triphasic can be classified as

i) The reaction, which occur only in the presence of co-solvent as biphasic system to the products with appreciable selectivity.

ii) The reactions which occur in the biphasic conditions but there is significant enhancement in reaction rate and product selectivity under triphasic conditions.

iii) In triphasic conditions other routes are favored compared to that exhibited in biphasic conditions.

iv) Reactions that do not occur in the presence of solvent can undergo in solvent free conditions at least to some extent.

The reactions that proceed by first pathway are the biphasic systems. The reactions through (ii) and (iii) route favor the triphasic systems. For the environmentally safer chemical transformations by reducing/removing toxic waste and by-products obtained from the chemical process, one of the major problems is the use of organic solvents, which are detrimental to nature [65,67]. In this consequence organic transformations

under solvent free (iv) conditions are attracting increasing attentions. Solvent free [66,67] oxidative transformations either do not take place or occur to an insignificant extent with products using solvents.

1.13. Redox molecular sieves

Molecular sieves containing redox active metals are used as active and selective catalysts for oxidative transformation of organic molecules [68]. The advantage over soluble metal compounds which are used as homogeneous catalysts or as stoichiometric amounts is that the use of redox molecules as heterogeneous catalysts avoids contamination of the effluents, which are becoming increasingly difficult to dispose. The versatility of redox molecular sieves over other heterogeneous catalysts is that it is possible to influence which substrate molecules approach the active site by choosing a suitable combination of molecular sieve and solvent [57]. The molecular sieves can be viewed as a second solvent, as it selectively extracts the substrate molecules from the bulk solvent. Which substrate molecules are selectively extracted is determined by the size and hydrophobicity of the pores of molecular sieves and substrate. Their properties such as pore dimensions, hydrophobicity, acidity and basicity can be tailored over abroad range allowing the preparation of highly sensitive catalysts and are effective with clean and economical oxygen donors such as 30% aqueous hydrogen peroxide [68].

Zeolites or zeotypes molecular sieves consisting of regular array of pores of molecular dimensions 4-13 Å, the incorporation of redox metals into them produces

potential heterogeneous oxidation catalysts. Metal incorporated molecular sieves of MFI and MEL type structure have been investigated for selective oxidation reactions like epoxidation, hydroxylation, oxyfunctinalization of alkanes, ammoxidation, sulfoxidation, etc [68]. Although zeolites showed very high activity and selectivity they could be effective only in the oxidation of small molecules due to the small pore size of these materials (5.3 x 5.5 Å). Because of that a considerable amount of research dedicated for the preparation of large pore metallosilicate molecular sieves resulted in structures like Ti-substituted beta zeolite with a beta structure (7.6 x 6.4 Å), enables the epoxidation of long chain alkanes [69-71].

However to catalyze even bulkier substrates, development of mesoporous molecular sieves like MCM-41 with unique physical properties enhanced the incorporation of redox species by isomorphous substitution or by grafting or by anchoring. Mesoporous Ti-MCM-41 and Ti-HMS were found to be effective in the epoxidation of norbornene with TBHP and oxidation of 2,6-di-tert butyl phenols with aqueous H_2O_2 respectively [45,72]. Ti- grafted MCM-41 was found to be active for the selective epoxidation of cylohexene and α-pinene using TBHP as oxidant. Vanadium substituted in the porous framework of MCM-41, were highly active and selective for the partial oxidation of cyclododecane and 1-naphthol with H_2O_2 as oxidant [46,73-76]. Likewise Cr incorporated mesoporous silicates are found active as oxidation catalysts [47]. Although, the nature of catalytic properties depends upon the nature of metal sites, structure and sorption properties of molecules also produce some effects on its activity and further in the selectivity.

1.14. Oxidation of ethyl benzene and diphenyl methane

Oxidation reactions involving hydrocarbons are frequently important components in many industrial processes. The selective partial oxidation of alkyl aromatics is commercially done using complex multistep processes with the formation of considerable amounts of wastes. For these alternative and cleaner process with both economical and environmental feasibility are sought.

The catalytic oxidation of ethyl benzene and diphenyl methane to their keto derivatives is a versatile route for the synthesis of many fine chemicals. Aromatic ketones such as acetophenone and benzophenone are important intermediates for drugs as well as in the pharmaceuticals [77]. Earlier, synthesis of such ketones are performed by the oxidation reaction of the methylene groups attached to the aromatic ring using stoichiometric quantities of oxidizing agents like $KMnO_4$ or $K_2Cr_2O_7$, [78, 79]. An alternative route for the production of such keto compounds is Friedel-Crafts acylation reaction of aromatics by acid halide/anhydride, using stoichiometric amounts of corrosive $AlCl_3$ catalysts. In the above two processes, the large amount of waste produced and the usage of stoichiometric amount of catalysts makes the process unacceptable. Hence in the production of many fine as well as bulk chemicals, traditional processes are environmentally unacceptable because they involve multi-step synthesis procedures as well as generates large quantities of corrosive waste as by products. Thus, it is of interest to develop solid redox catalyst to perform these reactions over environmentally benign oxidizing agents like H_2O_2 or TBHP, where water and alcohol are produced as by products. Chromium-containing catalysts are used earlier for the oxidation of ethyl benzene while a proper comparison with the well-studied mesoporous materials (Ti-

MCM-41, V-MCM-41) is rare in the literature, especially over diphenyl methane [80, 81]. Thus the single step synthesis of keto products by the catalytic oxidation of ethyl benzene as well as diphenyl methane using metal- containing mesoporous materials is highly appreciable and attractive.

Objectives of the present study

- To synthesize and characterize silicate MCM-41 (Si-MCM-41), titanium, vanadium and chromium modified MCM-41 by direct hydrothermal method (M-MCM-41) for the oxidation of ethyl benzene and diphenyl methane, as this reaction is highly limited in zeolites due to its small pore diameter.

- To study the effect of the nature of metal in the structure and morphology of the modified mesoporous catalysts.

- To study the catalytic activity of metal modified mesoporous catalysts for the industrially important catalytic oxidation of ethyl benzene and diphenyl methane.

- To optimize various reaction parameters like molar ratio, solvents, temperature, oxidants, catalyst amount, etc to get better conversion and selectivity.

- To study the heterogeneity of metal containing catalysts by various leaching experiments.

CHAPTER II
EXPERIMENTAL

The performance of a catalyst depends on the preparation method, its pretreatment conditions, and nature of the precursor materials apart from its reaction parameters. This chapter deals with the detailed description for the synthesis of metal substituted MCM-41 (M-MCM-41, M= Ti, V and Cr) and their catalytic activity measurement in the oxidation reaction of ethyl benzene and diphenyl methane. Also in this chapter the fundamental principles and experimental details of different spectroscopic and analytical techniques used for the characterization of the various mesoporous materials synthesized are also described.

2.1. Materials used

1) Fumed Silica (Aerosil, Aldrich)
2) Cetyl trimethyl ammonium bromide (CTMABr, 99%, Loba Chemie)
3) Sodium hydroxide (99%, Merck)
4) Titanium isopropoxide ($Ti(OPr)_4$, Aldrich)
5) Vanadyl sulfate hydrate ($VOSO_4.3H_2O$, 99.9%, Aldrich)
6) Chromium Nitrate ($Cr(NO_3)_3$, Loba Chemie)
7) Ethyl Benzene (Lancanster)
8) Diphenyl Methane (Aldrich)
9) Hydrogen peroxide (aqu.30wt.%, Loba Chemie)
10) Acetonitrile (Merck)

2.2. Preparation of catalysts

2.2.1. Synthesis of Si-MCM-41

A silicate MCM-41 was prepared from a gel having the molar composition

SiO_2 : 0.3 TMAOH : 0.25 CTMABr : 120 H_2O

The gel mixture was autoclaved in a Teflon lined stainless steel autoclave kept in an oven under static condition, at 100 ^oC for the crystallization under autogeneous pressure, for 3 days. The solid product obtained was filtered, washed several times with distilled water and dried to get as-synthesized Si-MCM-41.The surfactant was removed by calcination at 500 ^oC for 5 h in air to get porous Si-MCM-41 material.

2.2.2. Synthesis of M-MCM-41 by hydrothermal method (M= Ti, V and Cr)

Ti-MCM-41, V-MCM-41 and Cr-MCM-41 were synthesized hydrothermally using a gel composition of SiO_2: 0.02M: 0.2CTMAB: 0.45NaOH: 120H_2O; where M = Ti, V, and Cr. In a typical synthesis procedure, required quantity of metal source was added slowly to a mixture of 2.4 g fumed silica, 2.88 g CTMAB, and 88 g H_2O under vigorous stirring. After 2 h, 0.72 g NaOH was added slowly and the pH of the gel mixture was adjusted between 10.5-11.5 depending on the metal source used, and the mixture was stirred for 4 h under room conditions. For titanium butoxide, isopropyl alcohol was used as the dispersing medium instead of water. The gel obtained was sealed into Teflon-lined steel autoclaves and heated at 100 ^oC for 3 days. For comparison, a silica polymorph was also prepared by a similar method, but with out the addition of metal salts. The solid product thus obtained was recovered by filtration,

washed with water (x5), and dried at 100 ^{o}C for 3 h. Finally, the materials were calcined at 540 ^{o}C in air for 5 h to obtain the porous M-MCM-41 materials.

2.3. Catalyst Characterization

Catalyst characterization is a lively and a highly relevant discipline in the field of catalysis. The nature of the performance can be greatly appreciated if one knows as many of its physical properties as possible. The nature of the active phases of vanadia may differ on loading and on its treatment conditions. So these factors are screened with the help of different complementary characterization techniques.

2.3.1. X-Ray diffraction

Powder X-ray diffraction analysis helps to identify the structure, phase purity, degree of crystallinity, unit cell parameter, crystallite size and also the kinetics of crystallization of various molecular sieves. A phase is assumed to be pure when the X-ray pattern matches with that of the reported one and some or all peak positions are differing with those of the reported structures in the case of new structures. Compared to microporous materials, which show characteristic peaks in the 2 theta range of 5-50^{o}, the mesoporous materials exhibits characteristic peaks in the low angle region between 1.5-10^{o} (2 theta). A fixed wavelength is chosen for the incident radiation and the diffraction pattern is obtained by observing the intensity of the scattered radiation as a function of the scattering angle 2θ. The d spacing can be found from the Braggs equation, which relates d spacing and scattering angle with the wavelength of the incident radiation and can be stated as

$$\mathbf{n\,\lambda = 2d\sin\theta}$$

Where, d is the lattice spacing, θ is the measuring angle, λ is the wavelength of X-rays used (1.5414 Å).

The present investigation of phase identification was performed on a Rigaku model D-Max III VC; Japan with Ni filtered Cu-K∝ radiation having curved graphite crystal monochromator and NaI scintillation counter.

2.3.2. Surface area measurement

Measurement of surface area of solid catalyst can be done by adsorption using the well-known BET method proposed by Brauner, Emmet and Teller [82], which assume the dynamic equilibrium between the adsorbed molecules and the molecules in the gas phase. They differed from Langmuir in assuming that the adsorption is multilayer where, the first layer is the truly adsorbed layer and subsequent layers are the condensed ones. The BET plot obtained by volumetric method is generally used for the measurement of the surface area of the catalyst. From the BET equation

$$\mathbf{P/V\ (P_o - P) = 1/\ C\ Vm + (C - 1)\ P/\ C\ Vm\ P_o}$$

Where, P = adsorption equilibrium pressure

P_o = saturation vapour pressure of the adsorbate

V = volume of nitrogen adsorbed at pressure P

Vm = the volume of nitrogen necessary to form a mono layer on unit surface

C = BET constant

A plot of P/ V (P_o – P) verses P/P_o should give straight-line with slope of (C –1)/ Vm C and intercept of 1/ Vm C, from which the mono layer capacity Vm can be calculated. The monolayer volume of the adsorbate converted to NTP is related to the total surface as,

$$\text{Total surface} = Vm.\ N.\ Am.10^{-20} / 22414\ (m^2)$$

Where N = Avagadro number

Am = the cross sectional area of the adsorbate (for Nitrogen, Am= 16.2 $Å^2$).

The specific surface (m^2/g) is obtained by dividing total surface by weight (g) of the sample. The specific surface area, total pore volume and average pore diameter were measured by N_2 adsorption-desorption method using NOVA 1200 (Quanta chrome) instrument

2.3.2.1. Pore size distribution by BJH method

The pore size distribution of a carrier or a catalyst is usually presented in the form of a plot of increment of pore volume per increment of pore size versus pore size. In a typical method for the calculation of pore size distribution from nitrogen adsorption isotherms, a cylindrical pore model may be assumed, which further assumes open ended and absence of pore networks. The BJH method involves the area of the pore walls and uses Kelvin equation to correlate the partial pressure of nitrogen in equilibrium with the porous solid to the size of the pores where capillary condensation takes place.

The pore size distribution is obtained the analysis of adsorption isotherm. First the volumes desorbed from the sample at different partial pressure are converted to liquid volumes, then by the use of Kelvin equation core of the liquid in the capillary can be found out by the equation,

$$R\ T\ \ln (P/P_o) = -\ 2\ \sigma\ Vm/\ r_k$$

Where, R = gas constant

T = the normal boiling point of nitrogen

σ = surface tension of nitrogen at T

Vm = molar volume of nitrogen

Since multilayer adsorption usually accompanies the capillary condensation in the porous solid, the Kelvin equation will not give correct radius since the pore size will have been effectively reduced by the thickness of the adsorbed multilayer. The maximum radius will be filled by capillary condensation at pressure, P is therefore,

$$r_p = t + 2\sigma Vm/RT\ln(P/P_o)$$

The radius of the pore (r_p) is obtained by adding the value of film thickness (t). The value of t as a function of P/P_o has been estimated with non-porous materials of known surface area. At each value of P/P_o, the total volume of the pores (Vp) filled up can be found out. A plot of Vp against r_k is called structural curve. Pore size distribution can be obtained by plotting d Vp/ d rp. This plot will represent the relative abundance of the pores of various radii in the solid [83, 84].

2.3.3. Diffuse reflectance UV-Visible Spectroscopy

The UV-VIS spectroscopy allows the study of electronic transitions between orbitals or bonds in the case of atoms, ions or molecules in liquid or solid state. It is known to be a very sensitive and useful technique for the identification and

characterization of the metal ion co-ordination and its existence in the framework or extra framework position of metal containing molecular sieves. Electronic transitions are of two types and involve orbitals or levels localized in the same metal atoms or adjacent atoms. The first class includes metal centered transitions d-d and (n-1)d–ns (in transition elements), f-f and 4f-5d (in rare earth elements) and ns- np in the main group elements. The second class involves the charge transfer (CT) transitions from an occupied level centered on a donor atom to a vacant one on an acceptor. This class includes ligand to metal and metal to ligand charge transfer and transition between MOs in inorganic or organic molecules or ions either free or coordinated to a metal named intra ligand charge transfers or ligand centered in the latter case. The position of the ligand to metal charge transfer band depends on the ligand field symmetry surrounding metal center and the electronic transitions from to metal ion than for hexa coordinated one. For most isomorphously substituted microporous and mesoporous metallosilicate molecular sieves, transition in the UV region (200-400 nm) are of great importance than the transitions in the visible range. The present UV-Vis study was done on a Shimadzu UV-2101 PC spectrometer equipped with a diffuse reflectance attachment using $BaSO_4$ as the reference.

2.3.4. Electron Microscopy

Electron microscope is similar to light microscope used for the magnification of the tiny objects separated by very minute distance that cannot be resolved with the aid of human eye and is generally defined as a microscope in which beam of electrons is used to

form a magnified image of the specimen. The discovery that accelerated electron behave in vacuum just like light, which have wave length about 100,000 times smaller than that of light is made use in electron microscopy. Furthermore, electric and magnetic field have the same effect on glass lenses and mirrors on visible light lead to the use of the in electron microscope.

2.3.4.1. Scanning Electron Microscopy (SEM)

An atom consists of a heavy charged nucleus surrounded by a number of orbiting electrons. The incoming electrons can interact with nucleus and be back scattered with virtually undiminished energy. Or it can interact with the orbiting electrons, an electron may be ejected from the atom (secondary electrons), and the atom with one electron short restores the status quo by emitting its excess energy in the form of an X-ray quantum or light photon. All these phenomena are inter related and al of them depend to some extend to on the topography, the atomic number and chemical state of the specimen. The number of back-scattered electrons, secondary electrons and adsorbed electrons at each point of the specimen depends on the specimen's topography too much extends than other properties. These three phenomena are exploited to image the specimen surface. The electrons produced when primary electron strikes the specimen in a SEM is collected by a collector and counted by detector, turned to electrical signals in a monitor and sends to amplifier, which gives the images on screen and hence SEM is the most versatile and widely used tool to study the morphology and composition of biological and physical

materials. SEM micrographs of the samples were obtained on a JEOL-JSM-5200 scanning microscopy

2.3.4.2. Transmission electron microscopy

TEM gives information about the particle shape, size and size distribution. TEM is being extensively used for the identification of the shape of the supported metal catalyst and also for measuring the particle size. An electron lens system (electric or magnetic field) focuses the electron beam with very narrow cross section at the point at which it hits the specimen. The transmitted electrons pass through another set of electron optics and finally the magnified image is produced. The electron beam striking the specimen produces several other effects such that the sample emits photons, Auger electrons, back-scattered electrons, etc. Transmission electron microscopy uses the information carried out by transmitted electrons – unscattered as well as elastically and in elastically scattered. In the study of the supported metal catalysts the sample preparation is of most importance. The catalyst is ground to fine powder. It is then dispersed in a solvent and drop of this suspension is placed on carbon film, which rests on electron microscope grid. The grid was sieves woven from thin metal wire usually nickel or copper. The particle size distribution can be obtained from the plot of particle diameter verses number of particles, in the form of a histogram. For this at least hundred particles should be counted. By particle here means the small crystallites of which the larger aggregates or the catalyst pellet is composed. TEM was performed on a JEOL JEM-1200

EX instrument with 100 kV acceleration voltage to probe the mesoporosity of the material.

2.4. Catalytic activity measurements

2.4.1. Oxidation of ethyl benzene and diphenyl methane

Reactions were performed in a round bottom flask fitted with a water-cooled condenser using 30 wt.% aqueous H_2O_2 and 70 wt.% aqueous TBHP as oxidants. The reactant mixtures of substrate (Aldrich), oxidant (Loba Chemie) and acetonitrile (E-Merck) solvent were added to 100 mg of catalyst and heated at a constant temperature of 80 ^{o}C under magnetic stirring. The typical molar ratio of the reactants was; substrate:oxidant:solvent = 1:3:6 (Scheme 5). After reactions, the reaction mixture was cooled to room conditions and the catalyst was separated from the reaction mixture by centrifugation. The oxidized products were analyzed on a gas chromatograph (HP 6890) equipped with a flame ionization detector (FID) and a capillary column (5 μm cross linked methyl silicone gum, 0.2mm×50m). The products were further confirmed by GC-MS (Shimadzu 2000 A) and by injecting authentic samples.

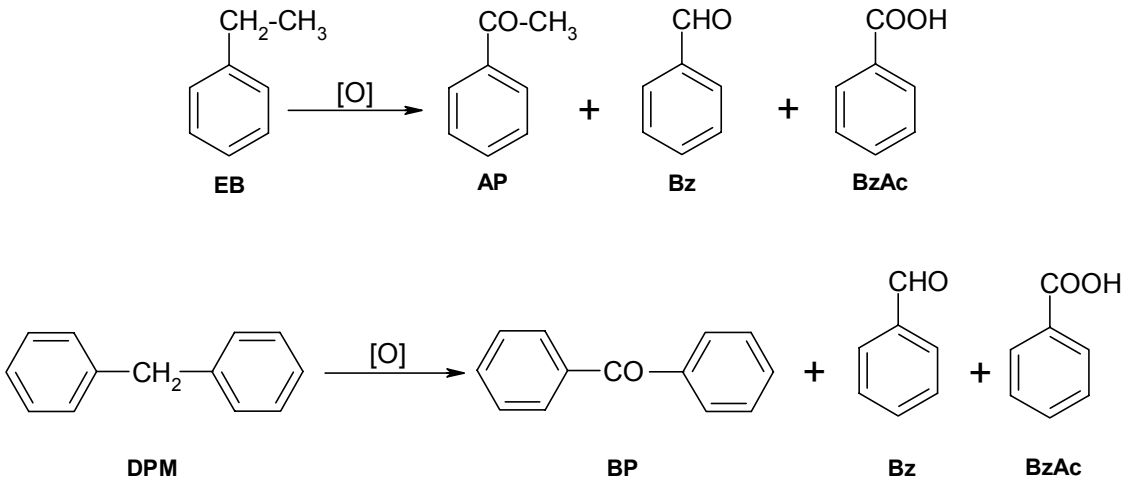
CH2-CH3
[O]
CO-CH3
CHO
COOH
EB
AP
Bz
BzAc
CH2
[O]
CO
CHO
COOH
DPM
BP
Bz
BzAc

Scheme 5

CHAPTER III

RESULTS AND DISCUSSION

This chapter describes the characterization of the as synthesized catalysts and its catalytic activity behaviour in the biphenyl hydroxylation reaction using the environmentally benign oxidant H_2O_2. The optimization and influence of various reaction parameters and the comparison of catalytic activity of the synthesized materials are also discussed briefly in this section.

3.1. Description of catalysts

1) Si-MCM-41 : Siliceous hexagonal mesoporous material.

2) Ti-MCM-41 : Titanium substituted mesoporous material.

3) V-MCM-41 : Vanadium substituted mesoporous material.

4) Cr-MCM-41 : Chromium substituted mesoporous material.

3.2 Characterization of Catalysts

3.2.1. X-Ray Diffraction

XRD patterns of all as-synthesized samples show four diffraction peaks corresponding to (100), (110), (200) and (210) reflexes, characteristic of ordered mesoporous materials with the hexagonal structure (Fig. 3.1 A). After calcination, a decreased intensity of the characteristic d_{100} peak with a corresponding disappearance of the long range ordered *210* peak is observed, showing a relatively well-ordered hexagonal structure for the materials (Fig. 3.1 B). A comparison among the M-MCM-41

mesoporous materials, in as-synthesized as well as in calcined state, shows that Ti- and Cr-MCM-41 shows a decreased intensity pattern than the V-MCM-41 material.

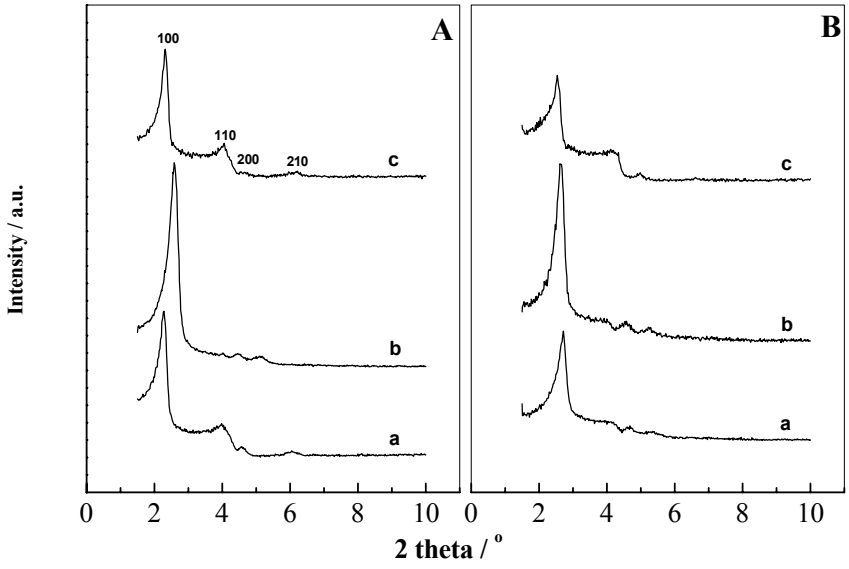

Fig. 3.1. X-ray diffraction patterns of, (A) as-synthesized M-MCM-41; (B) calcined M-MCM-41, where (a) Ti-MCM-41, (b) V-MCM-41 and (c) Cr-MCM-41.

Generally, in direct hydrothermal (DHT) methods, the incorporation of metal species in silica walls is feasible without the formation of M-O-M linkages [85]. Hence a better dispersion of metal species is expected under DHT methods than under similar metal concentrations prepared by impregnation methods or grafting methods. So in the present case, the formation of slightly oligomerized metal species may be the reason for the decreased intensity patterns of Ti- and Cr-MCM-41, than V-MCM-41 material. However, an increase in *d* spacing is observed for all the M-MCM-41 materials, than the silica polymorph, Si-MCM-41. These results are assigned for the incorporation of heteroatoms in the lattice positions, as M-O bond distances are longer than the Si-O bond

distances (Table 1) [86]. Absence of bands characteristic for crystalline TiO_2, V_2O_5 or Cr_2O_3 phase reveals that the metal ions were either atomically dispersed in the framework positions of MCM-41 or may exist in an amorphous dispersed form on the outside surface of mesoporous support.

3.2.2. Nitrogen adsorption-desorption isotherms

N_2 physisorption analysis are performed to confirm the structural ordering of the M-MCM-41 materials, since if the material had a regular pore structure it will show a steep increase in adsorption isotherm due to the capillary condensation. Isotherms of all samples show an inflection in the P/P_o range of ~0.2-0.4, characteristic of mesoporous solids of Type IV according to the IUPAC classification (Fig. 3.2). Moreover, a completely reversible adsorption-desorption isotherm is observed for all the developed M-MCM-41 samples. Generally, the inflection position in P/P_o depends on the diameter of the mesopores and its sharpness relates to the uniformity of mesopores. Accordingly, it can be seen that, V-MCM-41 posses the maximum pore size followed by Ti-MCM-41 and Cr-MCM-41. The textural parameters complied in Table 1, show that the materials posses a high surface area and larger internal void spaces, which in turn may help in an easy diffusion of the reactant species to the active metal sites residing inside the channel walls. The surface area of the catalysts, determined by the BET method, shows that all the catalysts exhibit high surface areas, typically in the range of 600-900 m^2g^{-1}. Interestingly, Cr-MCM-41 sample shows a large decrease in surface area than the V-MCM-41 and Ti-MCM-41 samples. Moreover, even though the Cr-O bond distance is larger than the Si-O bond distance, pore diameter of Cr-MCM-41 sample is also lower

than the Ti- and V-MCM-41 samples (Table 1) [85]. Thus the significant decrease in surface area and pore size of Cr-MCM-41 samples shows that a large part of the added chromium species reside outside the framework of the MCM-41 matrix; thereby decreasing the surface area as well as pore size drastically than the other two M-MCM-41 catalysts.

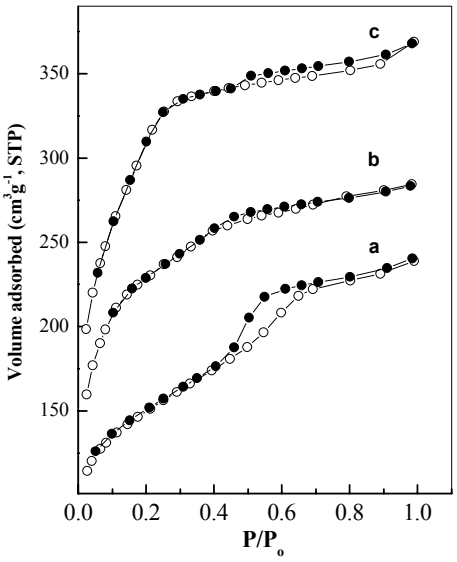

Fig. 3.2. N_2 adsorption-desorption isotherms of, (a) Ti-MCM-41, (b) V-MCM-41 and (c) Cr-MCM-41.

Table 1
Physico-chemical characteristics of M-MCM-41 materials

Sample	Cation radius (nm)	a_o values (nm) [a]	S_{BET} m^2g^{-1}	Pore volume V_p / ccg^{-1}	Pore diameter D_p / nm	M $2p_{3/2}$ B.E (eV) [b]
Si-MCM-41	0.041	3.7	980	0.57	2.1	103.3
Ti-MCM-41	0.068	3.8	901	0.55	2.2	459.3
V-MCM-41	0.049	3.9	905	0.53	2.2	~517.1
Cr-MCM-41	0.052	3.7	658	0.49	2.1	579.3

[a] $a_o=2d_{100}/\sqrt{3}$; [b] determined from XPS

Table 2
Metal content, color and percentage of surfactant groups in Si-MCM-41, Ti-MCM-41, V-MCM-41 and Cr-MCM-41 materials

sample	M/Si (ICP analysis)		color			weight loss (TG analysis)
	in gel	in product	as synthesized	calcined	hydrated	
Si-MCM-41	-	-	white	white	white	25
Ti-MCM-41	0.02	0.006	white	white	pale yellow	29
V-MCM-41	0.02	0.007	white	white	yellow	32
Cr-MCM-41	0.02	0.011	green	yellow	yellow	28

3.2.3. Thermogravimetric Analysis

TG-DTG/DTA analyses of as-synthesized M-MCM-41 materials show an almost identical thermal pattern as that of the corresponding silica polymorph, Si-MCM-41 material. The TGA patterns of Si-MCM-41 show a sharp weight loss below 100 ^{o}C corresponding to the loss of physisorbed water molecules while further decomposition patterns extend to 200-250 ^{o}C and to 300-350 ^{o}C, attribute for the combustion of the hexagonally packed surfactants (figure not shown). These results are supported from the DTA analysis, which show that the entire template including the water adsorbed on the hydroxyl groups is removed at a temperature of ~400 ^{o}C. However, a detailed examination shows that the percental weight loss of the surfactant is more in case of M-MCM-41 catalysts (~40%) than the corresponding silica polymorph (~35%). Further, it is noted that the percental weight loss also varies over M-MCM-41 samples and the weight loss observed are complied in Table 2.

3.2.4. Electron Microscopy

The particle size and morphology of Ti-MCM-41, V-MCM-41, and Cr-MCM-41 samples were determined by SEM analysis and are shown in Fig. 3.3 A. The formation of various periodic mesoporous materials starts with nucleation, which involves the surfactant-silicate interactions, and these interactions facilitate the assembly of the surfactant-silicate species in the desired morphology. However, the presence of foreign ions in the synthesis gel alter the structure directing action of the template and the attenuations further depends on the nature of metal source used. In accordance with this,

the micrographs show marked differences in the morphology of the samples after metal incorporation. The Ti-MCM-41 sample shows spongy structures (ca. ~3-5 μm in diameter), V-MCM-41 catalyst shows flower like structure (ca. ~2-3 μm in diameter), while Cr-MCM-41 shows agglomerated structures of ca. ~3-4 μm in diameter. The differences in SEM images thus illustrate that various metal ions can modify the morphological structure of the MCM-41 surface considerably [87]. In addition, TEM analysis shows an ordered mesopore structure for the Ti- and V-MCM-41 material, while Cr-MCM-41 shows a disordered structural pattern and are shown in Fig 3.3 B.

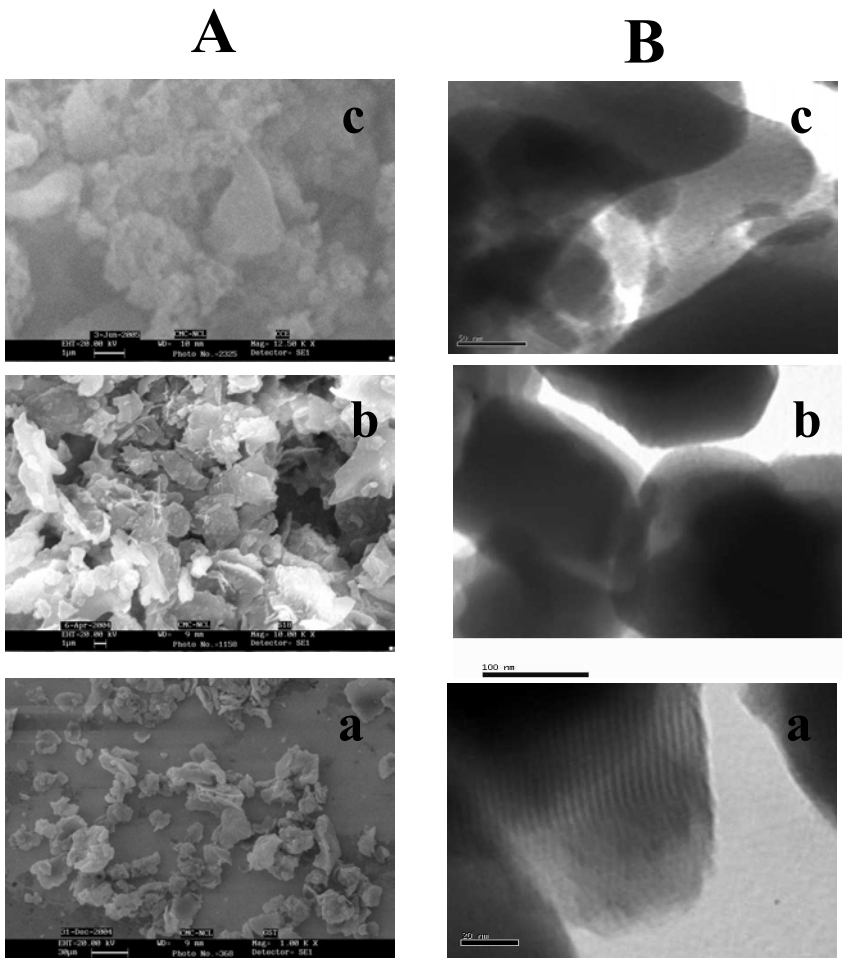

Fig. 3.3. SEM images (A) and TEM images (B); where (a) Ti-MCM-41, (b) V-MCM-41 and (c) Cr-MCM-41.

3.2.5. Diffuse reflectance UV-Vis spectroscopy

Diffuse reflectance UV-Vis (DR UV-Vis) spectroscopy is a useful technique to obtain information about the coordination environment and oxidation states of various redox metals on porous supports. Si-MCM-41 shows a band at 220 nm typical for the siliceous materials but new bands are appeared in the range of 200-600 nm after metal incorporation and the shift in wavelength depends on the nature of the metal species introduced into the MCM-41 matrix (Fig. 3.4). Usually, direct information about the oxidation state and dispersion of metal species can be interpreted from the color changes of the materials, during various treatment conditions (eg. hydration effects). The as-synthesized Ti-MCM-41 and V-MCM-41 are white colored, while Cr-MCM-41 is green in color. However, after calcination and exposure to ambient conditions, the color of V-MCM-41 and Cr-MCM-41 turns yellowish (Table 2). The display of colors before and after calcination shows the possible change in the coordination state of metal species inside the MCM-41 matrix. The change further indicates that a major part of metal atoms are on the wall channels so that water molecules can easily access the metal site for further coordinations. In detail, for Ti-MCM-41 catalyst, UV-Vis indicate a broad band between 210-300 nm, centered around 250 nm. Earlier literature reports over TS-1 catalyst show a peak maxima at 210 nm, attributed to the low energy charge transfer (CT) transition between tetrahedral oxygen ligands and the central Ti^{4+} ions, indicating the framework incorporation of titanium ions in the inorganic matrix [88]. However, for M41S related materials such sharp absorption bands are not observed at lower Si/Ti ratios while a shift of this band from 210 nm to ~250-260 nm is usually noted. Hence in the

present case, the shift of the band to higher wave number indicates that titanium exists as distorted tetrahedral environments inside the MCM-41 matrix or as octahedrally coordinated titanium sites, due to the possible hydration effects (Scheme 6A). However, the absence of band after 300 nm proves well the absence of anatase phases under the present synthesis procedures. For V-MCM-41 sample the color changes observed after calcination is due to the modification in the oxidation state of vanadium (V^{5+}) from the isolated tetrahedral coordination (T_d, ~260 nm) to its distorted octahedral coordination ($O_{h,}$, ~320-360 nm) by contacting with water molecules in the atmosphere (Scheme 6B). Thus the presence of higher coordinated metal sites in case of titanium and vanadium indicates the less crystallographic order in the pore walls and/or to the possible hydration effects, due to the high surface area as well as large pore channels of the MCM-41 matrix. DR UV-Vis spectrum of calcined Cr-MCM-41 sample shows the presence of sharp bands at 260 nm and 350 nm with a shoulder at 450 nm. The bands at 260 nm and 350 nm are assigned to the O to Cr (VI) charge transfer transitions of chromate species while the band centered at 450 nm is assigned to the charge transfer bands associated with the dichromate or polychromate species [89]. This result indicates that the major species formed on the Cr-MCM-41 sample is monochromates, with minor amounts of dichromates as well as polychromate species (Scheme 6C).

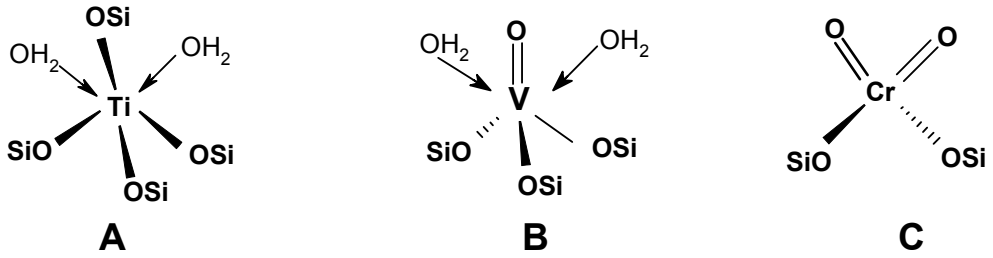

Scheme 6

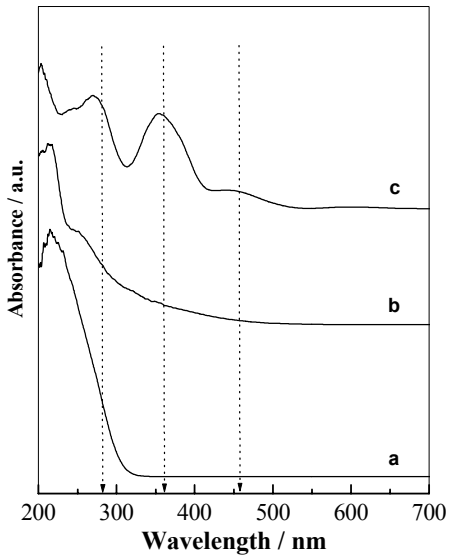

Fig. 3.4. DR UV-Vis spectra of calcined M-MCM-41 samples; where (a) Ti-MCM-41, (b) V-MCM-41 and (c) Cr-MCM-41.

3.2.6. Electron paramagnetic resonance (EPR)

The X band ESR spectra of as-synthesized vanadium- and chromium-containing mesoporous materials, recorded at room temperature, are given in Fig. 3.5. ESR analysis of Ti-MCM-41 samples showed no signals, which reveals the +4 oxidation state of titanium (diamagnetic nature) in the MCM-41 matrix [90]. As-synthesized V-MCM-41 sample (V^{4+}, d^1) exhibits the characteristic eight-line hyperfine splitting (hfs) patterns due to the interaction of the unpaired electron with the nuclear spin of the ^{51}V nuclei. The well resolved hyperfine splitting patterns obtained for the V-MCM-41 sample indicates that the $(VO)^{2+}$ ions are dispersed inside the pore channels of MCM materials and the observed g values (g_{η} = 1.945, $g_{\perp}$ = 1.997) and the hyperfine coupling constants (A_{η} =

185 G and $A_{\perp}$ = 68 G) are in agreement with the values for $(VO)^{2+}$ ions with a distorted pseudo octahedral coordination [91]. The ESR spectrum of as-synthesized chromium-containing mesoporous silica shows a broad peak with g_{eff} ~1.98, indicating the presence of trivalent chromium (Cr^{3+}) in octahedral coordination and are in accordance with the earlier results [89].

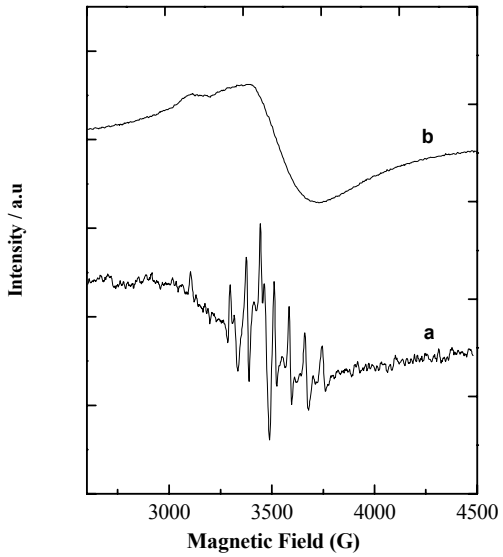

Fig. 3.5. ESR spectra of as-synthesized M-MCM-41 samples (a) V-MCM-41 and (b) Cr-MCM-41.

3.3. Catalytic activity measurements

Various characterization techniques reveal that, titanium-, vanadium- and chromium- get introduced into the silica framework and hence the materials were screened in the oxidation reaction of ethyl benzene (EB) and diphenyl methane (DPM) using aqueous H_2O_2 and TBHP as oxidants. As expected, an increase in the molar ratio

(1:1 to 1: 3 between substrate and oxidant) and temperature (60 to 80 ^{o}C) had a positive effect in the conversion of aromatics as well as in the selectivity to the desired keto derivatives. Since the product of importance is the keto compound, the catalysts were optimized at a substrate: oxidant ratio of 0.33 as well as at a higher temperature of 80 ^{o}C. Contrary to the reports over Mn-MCM-41 catalysts, in ethyl benzene oxidation reaction, we noted mainly the presence of three oxidized products-viz. benzaldehyde, acetophenone and benzoic acid and the results over TBHP is approximately three times lower than H_2O_2 [92]. These results can be explained in two folds. On one hand, the interaction of aqueous H_2O_2 will be more on the defect sites of the hydrophilic mesoporous material and thus can detach some of the metal species residing on extra framework positions to form soluble homogenous active metal species. On the other hand, the lesser percentage of active oxygen content in TBHP oxidant explains its lower activity values. Fig. 3.6 A shows the relationship between reaction time and conversion of ethyl benzene over various metal-substituted mesoporous catalysts, using aqueous H_2O_2 (30 wt.%) as oxidant. The formation of oxidized derivatives arises due to the well utilization of H_2O_2 by the active metal sites prevailing inside the pore channels of MCM-41 and the differences in the activity of M-MCM-41 samples depend on the nature of the transition metal introduced. These results are supported by the almost null activity of the parent silica support and thus the enhanced catalytic activity of the metal-containing catalysts arises unambiguously due to the presence of active metal species present in the support. The catalytic activity of metal-substituted mesoporous materials, in ethyl benzene oxidation reaction, follows the order, V-MCM-41>Ti-MCM-41>Cr-MCM-41 (Fig. 3.6 A). However, the selectivity to the desired keto derivative (acetophenone)

follows the order Ti-MCM-41>Cr-MCM-41>V-MCM-41 and it is interesting that Ti-MCM-41 shows a ketone selectivity of ~80%. Generally, the variation in activity and selectivity depends on dispersion as well as the coordination of the metal in the framework of porous materials. These factors further influence the nature of substrate and oxidant interaction with the metal sites. Hence it is reasonable that the decreased selectivity towards keto compounds in vanadium- and chromium- catalysts relates to the greater percentage of extra framework metal species, while for Ti-MCM-41 the decreased percentage of extra framework metal species may limits over oxidation process and thereby maintain the higher selectivity to acetophenone.

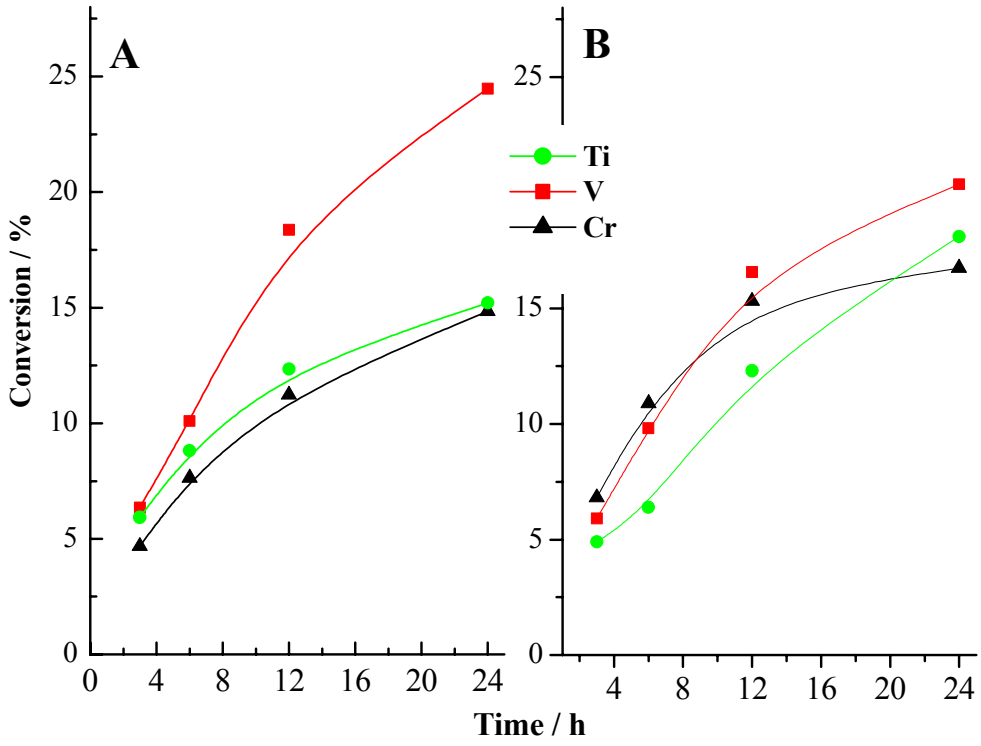

Fig. 3.6. Influence of reaction time in the conversion of, (A) ethyl benzene and (B) diphenyl methane, where (●) Ti-MCM-41, (■) V-MCM-41 and (▲) Cr-MCM-41.

Results obtained from the oxidation of diphenyl methane (DPM) over metal-containing mesoporous materials are shown in Fig. 3.6 B. The nature of oxidant on DPM conversion over M-MCM-41 catalyst also shows that TBHP is almost inactive under the present reaction conditions. However, changing the oxidant from TBHP to H_2O_2 increases the conversion drastically and hence aq. H_2O_2 was used as an oxidant for further experiments. As obtained over ethyl benzene, it is noted that the DPM conversion follows the order V-MCM-41>Ti-MCM-41≥Cr-MCM-41 (Fig. 3.6 B), while selectivity towards benzophenone follows the order Ti-MCM-41>V-MCM-41>Cr-MCM-41. Hence, irrespective of the substrate molecule, V-MCM-41 shows better conversion rates while the selectivity to the desired keto products, viz. acetophenone and benzophenone is maximum over Ti-MCM-41 catalyst.

Catalysis by early transition metals like Ti (IV), V (V) or Cr (VI) involves a metal peroxo intermediate species because of the vacant *d* orbitals. It is known that the catalytic performance of transition metal species depends on the outer *d* electron density, since lower the *d* electron density the ability of metal species to activate the oxidant species is higher [93]. Hence if such an assumption is followed for accounting the catalytic performances of M-MCM-41 catalysts an almost similar result must be obtained over all the catalyst systems. However, the oxidation of aromatics follows different over M-MCM-41 catalysts and hence it is relevant that some other factors like the textural properties also plays a vital role in the catalytic activity of the materials. Because of this reason, it is interesting to note that in as-synthesized as well as in calcined forms, V-MCM-41 catalyst shows a better structural pattern than the other two M-MCM-41 catalysts. Indeed, V-MCM-41 catalyst shows better conversion in the oxidation of ethyl

benzene and diphenyl methane than Ti-and Cr-MCM-41 catalysts. Such a result unambiguously shows that, even though active redox sites are introduced over Si-MCM-41 matrix, the structural features of the final mesoporous materials also affect the catalytic performances. Hence, apart from the nature of metal sites, the variation in catalytic activity between Ti-, V- and Cr-containing catalysts may also relates to the difference in the mesopore structural ordering, since in a regular pore channel all the active sites are well exposed for the diffused reactant species to react than over a disordered mesoporous material [87].

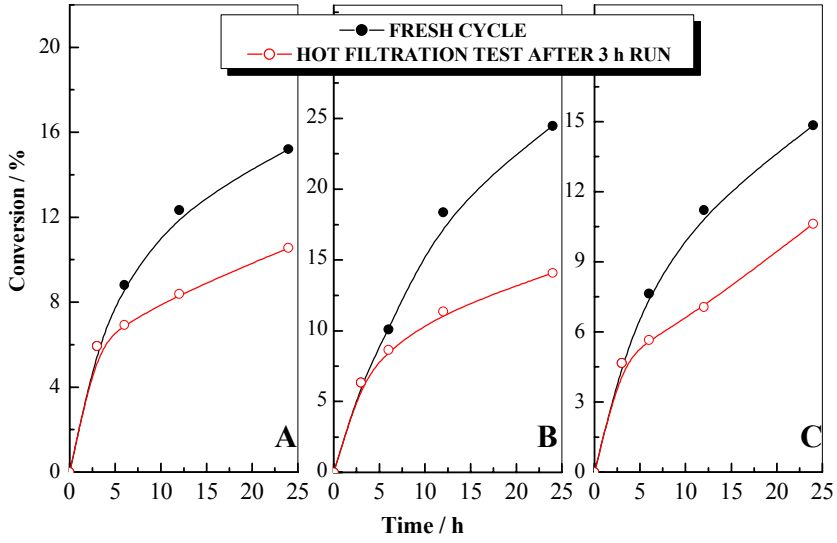

Fig. 3.7. Hot filtration experiments performed over M-MCM-41 catalysts in the ethyl benzene oxidation reaction, (A) Ti-MCM-41, (B) V-MCM-41 and (C) Cr-MCM-41, where (●) for fresh cycle and (○) for filtration after 3 h run.

Literature reveals that vanadium- and chromium-containing mesoporous materials show the leaching of active metal species during reactions and hence it is important to verify whether the enhanced catalytic activity may arise from such homogeneous leached

metal species [88, 89]. For that, strictly hot filtration experiments are performed since at lower temperatures the leached metal species can readsorb to the solid catalyst surfaces. Accordingly, the resubmission of the hot filtrate under the reaction conditions show that all the M-MCM-41 catalysts shows the leaching of active metal sites and the extent of leaching (in ethyl benzene oxidation reaction) follows the order, Cr-MCM-41>>V-MCM-41>Ti-MCM-41 (Fig. 3.7). Moreover, hot filtration experiments performed in the diphenyl methane oxidation reaction shows that the removal of metal species during reaction follows, Cr-MCM-41>V-MCM-41>>Ti-MCM-41 (Fig. 3.8).

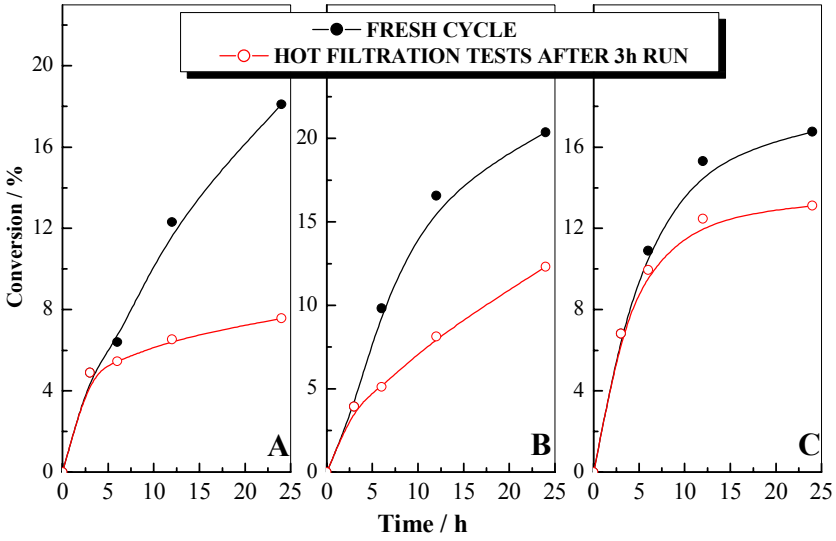

Fig. 3.8. Hot filtration experiments performed over M-MCM-41 catalysts in the diphenyl methane oxidation reaction, (A) Ti-MCM-41, (B) V-MCM-41 and (C) Cr-MCM-41, where (●) for fresh cycle and (○) for filtration after 3 h run.

Thus the present study demonstrates that, even though Cr-MCM-41 shows good catalytic performances, it arises from the leaching of loosely bound non-framework metal species, while for Ti-, V- MCM-41 catalysts the extent of leaching is limited and may

arise from the difference in the nature of coordination of metal species within the MCM-41 framework sites [Scheme 6]. Moreover, we had performed a second leaching study (hot filtration experiment) with the used Ti-, V- and Cr-MCM-41 catalyst (after repeated washing with dichloromethane and drying at 100 ^{o}C). Interestingly, even though the conversion gets decreased in the second reuse the extent of leaching decreased dramatically for all catalyst systems and for Ti-MCM-41 catalyst conversion gets essentially stopped after the removal of the catalyst. These results emphasizes the importance of performing leaching experiments over M-MCM-41 catalyst systems and shows that, even though titanium is tetrahedrally coordinated in titanosilicates a rigorous proof is needed in order to account for their exact catalytic activity. Moreover, structural ordering of the spent catalysts verified from XRD measurements shows that titanium- and vanadium- containing materials retain their structures while Cr-MCM-41 sample shows a more damaged structure and are in accordance with the above characterization results.

CHAPTER IV
SUMMARY AND CONCLUSIONS

The present study describes the synthesis, characterization and catalytic activity of metal containing mesoporous MCM-41 materials like Ti-MCM-41, V-MCM-41 and Cr-MCM-41. These materials were used as catalysts in the catalytic oxidation reaction of ethyl benzene and diphenyl methane. In the light of the above studies, the results obtained can be summarized as follows:

i) Chapter one describes the importance of catalysis on applied science with particular emphasis to catalysts as molecular sieves and thereby the need of mesoporous molecular sieves in catalysis. The different possible for he modification of mesoporous materials is briefly described, and the applications of ordered mesoporous materials are pointed out with particular emphasis to titanium, vanadium and chromium.

ii) Chapter two gives the experimental details of the synthesis of Si-MCM-41, Ti-MCM-41, V-MCM-41 and Cr-MCM-41 by direct hydrothermal method. This chapter also gives the experimental details and principle of various physicochemical characterization techniques used along with their potential catalytic applications.

iii) Chapter three presents the results obtained from various physicochemical techniques used in catalyst characterization. The detailed discussion of the physicochemical characteristics of the synthesized catalysts by means of XRD, UV-VIS, surface area by BET method, pore size distribution by N_2 adsorption-desorption isotherm, SEM, TEM, XPS, EPR, etc. In the second half of this chapter, the optimization of reaction parameters in the oxidation reaction of ethyl benzene and diphenyl methane are described.

Conclusions:

i) The catalysts used in this study i.e., Ti, V, Cr- modified MCM-41 can be synthesized by direct hydrothermal methods by careful tuning in the synthesis protocols. The results shows that V-MCM-41 materials synthesized by hydrothermal method have well-ordered mesostructures with long range ordering than the titanium and chromium containing mesoporous catalysts. Various characterization techniques highlight the difference in the nature of metal sites on the mesoporous framework.

ii) Metal modified and siliceous Si-MCM-41 materials showed surface area in the range of 1200-800 m^2/g and pore diameter in the range of 20-30 Å, which shows that all the materials synthesized are in the mesoporous range with very high surface area. The surface area results show that the decrease is more prominent for the Cr-MCM-41 catalyst.

iii) The diffuse reflectance UV-VIS spectra gives an account on the co-ordination environment and oxidation states of metal species from the charge transfer spectra of M-MCM-41 materials.

iv) The characterization of M-MCM-41 material by SEM and TEM reveal the formation of hexagonal mesoporous structures gets distorted over Cr-MCM-41 catalyst.

v) The optimization of reaction parameters concludes that, in the present reaction acetonitrile is the best solvent and an increase in hydrogen peroxide concentration as well as temperature directly influence the substrate conversions.

vi) A comparison of the catalytic activity of Ti-MCM-41, V-MCM-41 and Cr-MCM-41 shows that V-MCM-41 catalyst possess superior catalytic activity, which is indicative of the presence of the highly dispersed tetrahedral vanadia species in the silica framework with long-range order.

vii) Heterogeneity studies of the catalysts under reaction condition points out the fact that the nature of incorporation of metals on the silica framework greatly influences the heterogeneous nature of the catalysts and the heterogenity follows the order Ti-MCM-41>V-MCM-41>Cr-MCM-41.

REFERENCES

1. G. Ertt, H. Knozinger, J. Wetkemp, Handbook of Heterogeneous Catalysis, Wiley-VCH, 1997.
2. Ian. M. Campbell, Catalysis at Surfaces, Chappman and Hall, New York, 1988.
3. J.J. Burton, R.L. Garten, Advanced Materials in Catalysis, Academic Press, New York, 1977
4. B. Delmon, Coll, Scientific Bares for the Preparation of Heterogeneous Catalysis, Vol. I- VI, Elsevier, 1980.
5. K. S. W. Sing, D.H. Everett, R.H.W. Haul, L. Moscou, R.A. Pierotti, J. Rouquerol, T. Siemieniewska, Pure Appl. Chem. 57 (1985) 603.
6. D.W. Breck, Zeolites-Molecular Sieves, Wiley, New York, 1974.
7. R. Szostak, Molecular Sieves: Principles of Synthesis and Identification, Van Nostrand Reinfold, New York, 1989.
8. M. Taramasso, O. Forlani, G. Manara, B. Notari, U. K. Pat. 2023562 (1979).
9. B.L. Meyeres, S.R. Ely, N.A. Kutz, J.A. Kudak, E. V. Bosche, J. Catal. 91 (1985) 352.
10. B.D. Mc Nicol, G.T. Pott, J.Catal. 25 (1972) 223.
11. A. Bhaumik, R. Kumar, J. Chem. Soc., Chem. Commun. (1995) 349.
12. R. Kumar, P. Ratnaswamy, Catal. Lett. 22 (1994) 227.
13. Z. Gabelica, J.L. Guth, Stud. Surf. Sci. Catal. 49A (1994) 421.
14. M. Taramasso, G. Perego, B. Notari, U.S. Pat. 4410501 (1983).

15. A. Thangaraj, R. Kumar, S.P. Mirajkar, P. Ratnaswamy, J. Catal. 130 (1991) 1.

16. A.V. Ramaswamy, S. Sivasankar, P. Ratnaswamy, Catal. Lett. 22 (1993) 236.

17. B. Rakshe, V. Ramaswamy, A.V Ramaswamy, J. Catal. 163 (1996) 501.

18. M. E. Davis, C. Saldarriaga, C. Montes, J.M. Garces, J. A. Crowder, Nature 331 (1988) 698.

19. R.H. Jones, J. M. Thomas, J. Chen, R. Xu, Q. Huo, S. Li, Z. Ma, A.M. Chippindale, J. Solid State Chem. 102 (1993) 204.

20. C. T. Kresge, M. E. Leonowicz, W. J. Roth, J. C. Vartuli, J.S. Beck, Nature 359 (1992) 710.

21. J. S. Beck, J. C. Vartuli, W. T. Roth, M. E. Leonowicz, C. T. Kresge, K. D. Schmitt, C. T. W. Chu, D. H. Olson, E. W. Sheppard, S. B. Mc Cullen, J. B. Higgins, J. L. Schlenker, J. Am. Chem. Soc. 114 (1992) 10834.

22. C. J. Brinker, Curr. Opin. Solid State Mater. Sci. 1 (1996) 798

23. J. C. Vartuli, C. T. Kresge, W. J. Roth, S. B. Mc Cullen, J. S. Beck, K. D. Schmitt, M.E. Leonowicz, J. D. Lutner, E. W. Sheppard, Advanced Catalysts and Nanostructured Materials: Modern Synthesis Methods, Academic Press, New York, 1996.

24. A. Sayari, Chem. Mater. 8 (1996) 1840.

25. J. Y. Ying, C. P. Mehnert, S. Wong, Angew. Chem. Int, Ed. 38 (1999) 56.

26. A. Corma, Chem. Rev. 97 (1997) 2373.

27. P. A. Winsor, Chem. Rev. 68 (1968) 1.

28. P. Ekwall, Advances in Liquid Crystals, Ed. G. H. Brown, Academic Press Inc : New York, 1971.

29. J. C. Vartuli, C. T. Kresge, M. E. Leonowicz, A. S. Chu, S. B. Mc Cullen, I. O. Johnson, E. W. Sheppard, Chem. Mater. 6 (1994) 2070
30. C. Y. Chen, S. L. Burkett, H. X. Li, M. E. Davis, Microporous Mater. 2 (1993) 27.
31. A. Steel, S. W. Carr, M. W. Anderson, J. Chem. Soc., Chem. Commun. (1994) 1571.
32. A. Monnier, F. Schuth, Q. Huo, D. Kumar, D. Margolese, R. S. Maxwell, G. D. Stucky, M. Krishnamurthy, P. Petroff, A. Firrouzi, M. Janicke, B. Chmelka, Science 261 (1993) 1299.
33. G. D. Stucky, A. Monnier, F. Schuth, Q. Huo, D. Margolese, D. Kumar, M. Krishnamurthy, P. Petroff, A. Firouzi, M. Janicke, B. F. Chmelka, Mol. Cryt. Liq. Cryt. 240 (1994) 187.
34. A. Firouzi, D. Kumar, L. M. Bull, T. Besier, P. Sieger, Q. Huo, S. A. Walker, J. A. Zasadzinski, C. Glinka, J. Nicol, D. Margolese, G. D. Stucky, B. F. Chmelka, Science 267 (1995) 1138.
35. R. K. Iler, The Chemistry of Silica, Wiley, New York, (1979).
36. H. P. Lin, C. Y. Mou, J. Cluster Sci. 10 (1999) 271.
37. H. P. Lin, S. Cheng, C. Y. Mou, J. Chin. Chem. Soc. 43 (1996) 375.
38. Z. Zhang, Y. Han, L. Zhu, R. Wang, D. Zhao, F. S. Xiao, Angew. Chem. Int. Ed. 40 (2001) 1258
39. P. J. Bruinsma, A. Y. Kim, J. Liu, S. Baskaran, Chem. Mater. 9 (1997) 2507.
40. H. Yang, N. Coombs, I. Sokolov, G. A. Ozin, Nature 38 (1996) 589.
41. R. Ryoo, C. H. Ko, R. F. Howe, Chem. Mater. 9 (1997) 1607.
42. A. Sayari, C. Danumah, I. L Moudrakowski, Chem. Mater. 7 (1995) 813.

43. C. F. Cheng, H. He, W. Zhou, J. Klinowski, J. A. S. Gonclves, L. F. Gladden, J. Phys. Chem. 100 (1996) 390.

44. A. Tuel, S. Gotier, Chem. Mater. 8 (1996) 114.

45. P. T. Tanev, M. Chibwe, T. J. Pinnavaia, Nature 368 (1994) 321.

46. K. M. Reddy, I. Moudrakoovski, A. Sayari, J. Chem. Soc., Chem. Commun. (1994) 1059.

47. N. Ulagappan, C. N. R. Rao, Chem. Commun. (1996) 1047.

48. D. Zhao, D. Gold Farb, J. Chem. Soc., Chem. Commun. (1995) 875.

49. S. L Burkett, S. D. Sins S. Mann, Chem. Commun. (1996) 1367.

50. M. H. Lim, C. F. Blanford, A. Stein, J. Am. Chem. Soc. 119 (1997) 4090.

51. P. Sutra, D. Brunel, J. Chem. Soc., Chem. Commun. (1996) 2485.

52. A. Corma, A. Martinez, V. Martinez-Soria, J. B. Monton, J. Catal. 153 (1995) 25.

53. G. Grubert, J. Rathousty, G. Schulz-Ekloff, M. Wark, A. Zukal, Microporous Mesoporous Mater. 22 (1998) 225.

54. R. Ryoo, Kim, J. Kim, S. Jun, Chem. Commun. (1997) 2225.

55. F. Schuth, Stud. Surf. Sci. Catal. 135 (2001) 1.

56. J. Liu, X. Feng, G. E. Fryxell, L. Q. Wang, A. Y. Kim, M. Gong, Ad. Mater. 10 (1998) 161.

57. R. A. Sheldon, CHEMTECH, 21 (1991) 566.

58. R. A. Sheldon, Top. Curr. Chem. 164 (1993) 21.

59. F. M. Menger, J. Am. Chem. Soc. 92 (1970) 5965.

60. A. F. M. Barton, Chem. Rev. 75 (1975) 731.

61. C. M. Starks, J. Am. Chem. Soc. 97 (1971) 195.

62. E. V. Dehmlow, Angew. Chem. Int. Ed. Engl. 13 (1974) 170.

63. S. L. Regan, J. Am. Chem. Soc., 97 (1975) 5956.

64. S. L. Regan, Angew. Chem. Int. Ed. Engl. 18 (1979) 421.

65. H. Molinari, F. Monttanari, S. Quici, S. L. Regan, J. Am. Chem. Soc. 101 (1979) 421

66. J. Ameto, Science, 259 (1993) 1538.

67. J. O. Metzer, R. Mahler, Angew. Chem. Int. Ed. Engl. 34 (1995) 902

68. I. W. C.E. Arends, R. A. Sheldon, M. Wallau, U. Schuchardt, Angew. Chem. Int. Ed. 36 (1997) 1144.

69. M. A. Camblor, A. Corma, A. Martinez, J. Perez-Pariente, J. Chem. Soc., Chem. Commun. (1992) 8.

70. A. Corma, P. Estev, A. Martinez, S. Valencia, J. Catal, 152 (1995) 18.

71. T. Blasco, M. A. Camblor, A. Corma, P. Estev, A. Martinez, C. Prieto, S. Valencia, J. Chem. Soc., Chem. Commun. (1996) 2367.

72. A. Corma, M. T. Navarro, J. P. Pariente, J. Chem. Soc., Chem. Commun. (1994) 147.

73. V. Parvulescu, B. L. Su, Catal. Today 69 (2001) 315.

74. A. Sayari, V. R. Karra, J. S. Reddy, I. Moudrokovsky, Mater. Res. Soc. Symp. Proc. 371 (1995) 81.

75. D. Wei. H. Wang, X. Feng, W. T. Chueh, R. Ravikovitch, M. Lybovsky, C. Li, Takeguchi, G. L Hallor, J. Phys. Chem. B. 103 (1999) 2113.

76. N. N. Trukhan, A. Y. Derevyankin, A. N. Schmakov, E. A. Pankshtis, O. A. Kholdeeva, V. N. Romanikov, Microporous Mesoporous Mater. 44/45 (2001) 603.

77. V.R. Choudhary, J.R. Indurkar, V.S. Narkhede, R. Jha, J. Catal. 227 (2004) 257.

78. C.F. Cullis, J.W. Ladbury, J. Chem. Soc. (1955) 2850.

79. J.H. Clark, A.P. Kybett, P. London, D.J. Macquarrie, K. Martin, J. Chem. Soc. Chem. Commun. (1989) 1355.

80. A. Sakthivel, S.E. Dapurkar, P. Selvam, Catal. Lett. 77 (2001) 155.

81. S.E. Dapurkar, A. Sakthivel, P. Selvam, New. J. Chem. 8 (2003) 1184.

82. S. Braunauer, P. H. Emmet, E. Teller, J. Am. Chem. Soc. 60 (1938) 309.

83. J. M. Thomas, W. J. Thomas, Introduction to the Principles of Heterogeneous Catalysis, Academic Press, London, 1967.

84. Charles N. Satterfield, Heterogeneous Catalysis in Practice, Mc Graw Hill, New York, 1980.

85. S. Shylesh, A.P. Singh, J. Catal. 228 (2004) 333.

86. V. Parvulescu, B.L. Su, Catal. Today 69 (2001) 315.

87. V. Parvulescu, C. Anastasescu, B.L. Su, J. Mol. Catal. A: Chem. 3919 (2003) 1.

88. W. Zhang, M. Froba, J. Wang, P.T. Tanev, J. Wong, T.J. Pinnavaia, J. Am. Chem. Soc. 118 (1996) 9164.

89. A. Sakthivel, P. Selvam, J. Catal. 211 (2002) 134.

90. K. Chaudhari, D. Srinivas, P. Ratnasamy, J. Catal. 203 (2001) 25.

91. M. Mathieu, P. Vander Voort, B.M. Weckhuysen, R.R. Rao, G. Catana, R.A. Schoonheydt, E.F. Vansant, J. Phys. Chem. B 105 (2001) 3393.

92. S. Vetrivel, A. Pandurangan, J. Mol. Catal. A: Chem. 217 (2004) 165.

93. H. Jing, Z. Guo, D.G. Evans, X. Duan, J. Catal. 212 (2002) 22.